THE JOURNAL OF BIOLOGICAL CHEMISTRY
Vol. 278, No. 21, Issue of May 23, pp. 18730–18737, 2003
Printed in U.S.A.

Relationships of Ligand Binding, Redox Properties, and Protonation in *Coprinus cinereus* Peroxidase*

Received for publication, November 26, 2002, and in revised form, February 25, 2003
Published, JBC Papers in Press, March 5, 2003, DOI 10.1074/jbc.M212034200

Chiara Ciaccio‡§, Antonella Rosati§¶, Giampiero De Sanctis‖, Federica Sinibaldi‡, Stefano Marini‡, Roberto Santucci‡, Paolo Ascenzi¶, Karen G. Welinder, and Massimo Coletta‡ ‡‡**

*From the ‡Department of Experimental Medicine and Biochemical Sciences, Università di Roma Tor Vergata, Via Montpellier 1, I-00133 Roma, Italy, the ¶Department of Biology, Università Roma Tre, Viale G. Marconi 446, I-00146 Roma, Italy, the ‖Department of Molecular, Cellular, and Animal Biology, Università di Camerino, Via F. Camerini 2, I-62032 Camerino, Italy, and the **Department of Biotechnology, Aalborg University, Sohngaardshol-msvej 49, DK-9000 Aalborg, Denmark*

The pH dependence of the redox potentials and kinetics for CO association and dissociation was determined between pH 3.0 and 13.0 at 25 °C for the wild-type *Coprinus cinereus* fungal peroxidase and for a site-directed mutant in which Asp^{245}, which is H-bonded to N^{δ} of the imidazole of the proximal His^{183}, was substituted with Asn. The determination of these functional properties allowed this information to be merged in a self-consistent fashion and to formulate for the first time a complete scheme employing the minimum number of groups required to describe the whole proton-linked behavior of both redox and ligand binding properties. The overall pH dependence can be accounted for by four redox- and ligand-linked groups. The proximal H-bond, which is strictly conserved in all peroxidases, will still be present in the site-specific mutant, but will no longer have an ionic character, and this event will bring about an alteration of redox equilibria and CO binding kinetics, envisaging a relevant role played by this H-bond also in modulating redox properties and ligand binding equilibria.

The importance of the protein moiety in controlling the functional behavior of the active site in hemoproteins is a widespread concept, even though different proteins seem to apply various strategies to accomplish this interrelationship. Thus, in the case of multimeric hemoproteins such as human hemoglobin, the functional control is mostly exerted through a ligand-linked quaternary conformational transition, which affects ligand binding kinetic and thermodynamic parameters in a ligand-dependent fashion (1, 2).

In the case of monomeric hemoproteins, the protein matrix plays important roles through residues that either limit the access of the ligand to the distal portion of the heme pocket (3–6) or constrain the conformation of the hemoprotein stereochemistry in the proximal portion of the pocket (7–9). In the case of myoglobin, the H-bond between Ser^{92} and N^{δ} of the proximal His^{93} appears to be of particular importance (9).

In the case of heme peroxidases, an invariant H-bond between N^{δ} of the proximal imidazole and an aspartate (10–15) has been proposed to play a central role in the functional modulation of different peroxidases (16–18). As a matter of fact, we have shown that substitution of the invariant proximal aspartate of manganese peroxidase has a relevant influence on the redox potentials of this enzyme (19), confirming the hypothesis previously formulated (17, 18).

Peroxidases are divided into three main structural classes. Class I refers to intracellular peroxidases of prokaryotic origin such as cytochrome *c* peroxidase. Class II includes secretory fungal peroxidases such as manganese peroxidase, lignin peroxidase, and *Coprinus cinereus* peroxidase. Class III contains secretory plant peroxidases such as horseradish peroxidase (16).

In the last few years, particular attention has been addressed toward fungal peroxidases, also favored by the x-ray resolution of the structural arrangement for several of them and by their potential industrial usefulness. Therefore, a detailed description of different functional aspects of this class of peroxidases may be of relevance for better insight into their structure-function relationship. In particular, analysis of the pH dependence of different functional properties provides information on the proton linkage relationships, which are relevant for the modulation of functional properties of the protein. Such an approach is very demanding with respect to analysis of individual functional features because it is constrained by the requirement of a general description with the minimum number of parameters. As a matter of fact, it is often difficult to reconcile data concerning spectroscopic, thermodynamic, and kinetic observations, which indeed reflect differing structural and functional aspects of the whole molecule.

In this study, we analyzed some of the functional proton-linked equilibria and kinetics observed in the fungal peroxidase from *C. cinereus* (which is indistinguishable from the *Arthromyces ramosus* peroxidase; therefore, we will refer to CIP[1] also when referring to structural information taken from the crystal structure of *A. ramosus* peroxidase). The crystal structures of both peroxidases have been solved (14, 20), and the protein from *C. cinereus* has been thoroughly characterized by spectroscopic techniques (21–23). This study has focused on the role of Asp^{245} H-bonded to the proximal His^{183} in the redox and ligand binding properties as a function of pH. Analysis of CIP and the site-directed mutant D245N provided insight into the proton-linked equilibria in the oxidized and reduced forms, according to Scheme 1.

* This work was supported by Grant COFIN MM03185591 from the Italian Ministero dell'Università e della Ricerca Scientifica e Tecnologica. The costs of publication of this article were defrayed in part by the payment of page charges. This article must therefore be hereby marked "*advertisement*" in accordance with 18 U.S.C. Section 1734 solely to indicate this fact.

This paper is dedicated to the memory of Prof. Eraldo Antonini on the occasion of the 20th anniversary of his death.

§ Both authors contributed equally to this work.

‡‡ To whom correspondence should be addressed. Tel.: 39-6-7259-6365; Fax: 39-6-7259-6353; E-mail: coletta@seneca.uniroma2.it.

[1] The abbreviation used is: CIP, *C. cinereus* peroxidase.

MATERIALS AND METHODS

Recombinant wild-type CIP and the D245N mutant were both constructed and expressed in *Aspergillus oryzae* (24), and the protein samples were purified and prepared as previously described (21). The reduced Fe(II) form was obtained by addition of a minimum volume of fresh sodium dithionite to a deoxygenated buffered solution.

Cyclic voltammeter measurements were carried out using an AMEL 433 multipolarograph. All redox potentials reported here refer to the normal hydrogen electrode. Direct current cyclic voltammograms were run in different buffers (see below) at a scan rate of 50 mV/s. A pyrolytic graphite electrode (AMEL) was the working electrode; a saturated calomel electrode (+244 mV *versus* the normal hydrogen electrode at 25 °C; AMEL) was the reference electrode; and a platinum ring was the counter electrode. The pyrolytic graphite electrode was modified as follows. A suitable amount of tributylmethylphosphonium chloride polymer bound (polystyrene cross-linked with 1% divinylbenzene) to anion-exchange resin was dissolved in dimethyl sulfoxide to a final concentration of 0.035% (w/v). 8 μl of this solution were then mixed with 12 μl of 1.6 mM CIP (or D245N) solution and deposited on the surface of a pyrolytic graphite electrode (2 mm diameter) previously polished using an alumina (0.3-μm particle size)/water slurry, followed by sonication in deionized water (25). The modified electrode was left to dry overnight under vacuum before measurements.

CO binding kinetics were measured employing a rapid-mixing stopped-flow apparatus (SX.18 MV, Applied Photophysics Co., Salisbury, UK) with a 1-ms dead time. The protein was kept in one syringe in a deoxygenated solution (N_2-flushed with the addition of sodium dithionite to a final concentration of 1 mg/ml) in very low ionic strength 1.0 mM sodium phosphate buffer (pH 7.0), and it was mixed with a higher ionic strength buffer (final $I = 0.15$) at the desired pH value and concentration of CO. Progress curves were recorded at several wavelengths to follow both the formation of the CO adduct (at 423 nm) and the disappearance of the unliganded form (at 437 nm).

CO dissociation kinetics were followed on a Jasco V-530 spectrophotometer recording the absorption spectrum in the 380–450 nm range. The protein was kept at pH 7.0 in 1.0 mM sodium phosphate buffer in the presence of slightly substoichiometric amounts of CO. The reaction started when the protein solution was mixed in a large excess of oxygenated reaction mixture at the desired pH (final $I = 0.15$) because the dissociation of CO was followed by a rapid oxidation of the peroxidase, which was detected by the change of the absorption spectrum.

All experiments were performed at 25 °C in 1.0 mM $CaCl_2$ employing the following buffer systems: 0.15 M sodium acetate (pH 4.0–5.5), 0.15 M sodium phosphate (pH 3.0–4.0 and 5.0–7.5), 0.15 M Tris-HCl (pH 7.5–9.0), 0.15 M sodium borate (pH 8.5–9.5), 0.15 M sodium bicarbonate (pH 9.0–10.5), and 0.15 M sodium carbonate (pH 10.0–13.0). No buffer-dependent effects were observed at overlapping pH values.

The pH dependence of the redox properties was analyzed according to Equation 1,

$$E_{obs} = E_0 \cdot \frac{\sum_{i=0}^{i=n} \prod_{r=0}^{i} \cdot K_{ar(ox)} \cdot [H^+]}{\sum_{i=0}^{i=n} \prod_{r=0}^{i} \cdot K_{ar(red)} \cdot [H^+]} \qquad \text{(Eq. 1)}$$

where E_{obs} is the observed redox potential at a given pH value; E_0 is the redox potential of the form present at very alkaline pH values; $K_{a(red)}$ and $K_{a(ox)}$ are the proton binding constants in the reduced and oxidized forms, respectively (such as $K_a = 10^{pK_a}$), outlining that, in Equation 1, $K_{a0} \cdot [H^+] = 1$; and n is the total number of protonating redox-linked groups. It must be pointed out that, in Equation 1, we use the formalism K_a to refer to the groups that are sequentially protonated as pH is lowered, as also depicted in Scheme 1; therefore, r follows this sequence, and $r = 1$ relates to the residue displaying the highest pK_a value. Equation 1 indicates that only residues that change their pK_a upon reduction (or oxidation) contribute to the pH dependence of the redox potential.

The pH dependence of the CO binding second-order rate constant was analyzed according to Equation 2,

$$k_{obs} = \sum_{i=0}^{i=n} k_i \cdot \frac{\prod_{r=0}^{i} K_{ar(red)} \cdot [H^+]}{\sum_{i=0}^{i=n} \prod_{r=0}^{i} K_{ar(red)} \cdot [H^+]} \qquad \text{(Eq. 2)}$$

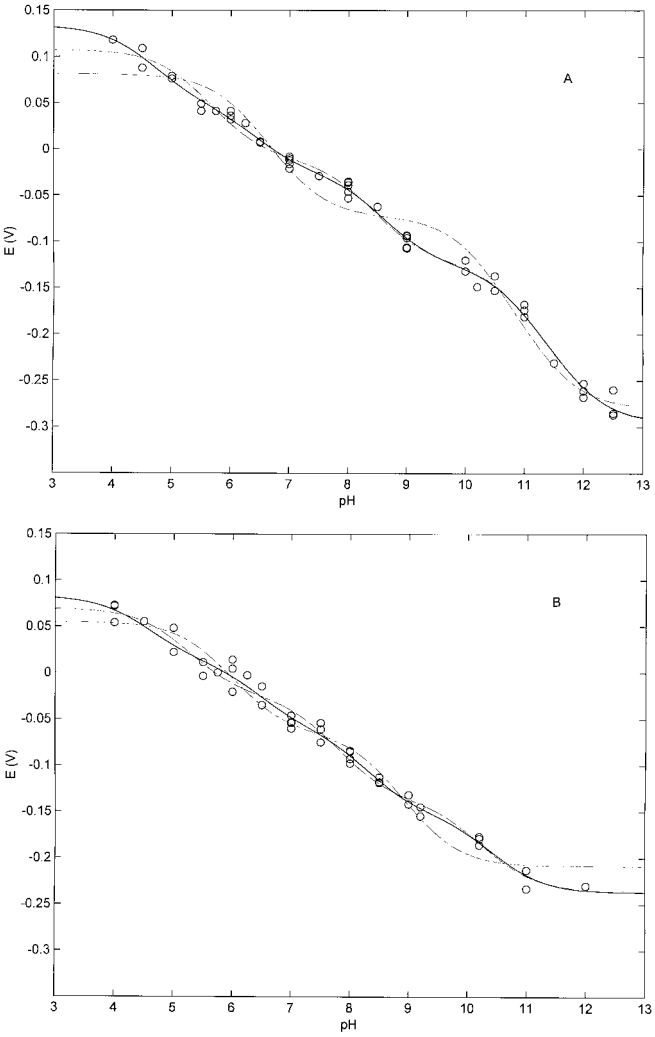

FIG. 1. *A*, pH dependence of the redox potentials for CIP at 25 °C. ——, nonlinear least-squares fitting of the data according to Equation 1 for $n = 4$ (values reported in Table I); – – –, nonlinear least-squares fitting of the data according to Equation 1 for $n = 3$; – - – -, nonlinear least-squares fitting of the data according to Equation 1 for $n = 2$. *B*, pH dependence of the redox potentials for D245N at 25 °C. ——, nonlinear least-squares fitting of data according to Equation 1 for $n = 4$ (values reported in Table I); – – –, nonlinear least-squares fitting of the data according to Equation 1 for $n = 3$; – - – -, nonlinear least-squares fitting of the data according to Equation 1 for $n = 2$. For further details, see "Results."

where k_{obs} is the observed CO binding second-order rate constant at a given pH value, k_i is the CO binding second-order rate constant of the ith-protonated species ($i = 0–4$), and all other symbols have the same meaning as described for Equation 1.

RESULTS

Fig. 1 shows the pH dependence of the redox properties of the wild-type peroxidase from *C. cinereus* (CIP) (Fig. 1*A*) and of the site-directed mutant D245N (Fig. 1*B*), in which Asn was substituted for Asp^{245}, which is H-bonded in CIP to the proximal His^{183}. Least-squares fitting of experimental data was carried out according to Equation 1, employing $n = 2$, 3, or 4. Least-squares fitting of the pH dependence of the redox properties employing $n = 2$ was clearly inadequate for both CIP and D245N (Fig. 1, *A* and *B*, – - – -), whereas $n = 4$ appeared to be only slightly better than $n = 3$. For a phenomenological description of the pH dependence of the redox properties of CIP and D245N, $n = 3$ might be satisfactory, using as few parameters as possible. Data from fitting according to $n = 3$ and 4 are reported in Table I both for CIP and the D245N mutant.

TABLE I
pK_a values for the redox-linked protonating groups in CIP and D245N from the fitting of the pH dependence of the redox potentials according to Equation 1 employing n = 3, 4

	CIP		D245N	
	$n = 3$	$n = 4$	$n = 3$	$n = 4$
$pK_{a1(ox)}$	11.98 ± 0.14	12.00 ± 0.15	10.61 ± 0.14	10.74 ± 0.13
$pK_{a2(ox)}$	8.84 ± 0.16	8.98 ± 0.16	8.21 ± 0.17	8.65 ± 0.16
$pK_{a3(ox)}$	6.09 ± 0.15	4.79 ± 0.18	5.62 ± 0.14	4.80 ± 0.16
$pK_{a4(ox)}$		6.71 ± 0.14		6.66 ± 0.12
$pK_{a1(red)}$	10.71 ± 0.14	10.75 ± 0.16	9.90 ± 0.13	10.12 ± 0.12
$pK_{a2(red)}$	8.02 ± 0.16	8.24 ± 0.17	7.38 ± 0.17	7.97 ± 0.17
$pK_{a3(red)}$	5.22 ± 0.14	6.10 ± 0.18	4.91 ± 0.15	6.12 ± 0.13
$pK_{a4(red)}$		4.21 ± 0.15		4.31 ± 0.11
$E_0(V)$	−0.294 ± 0.024	−0.295 ± 0.033	−0.235 ± 0.021	−0.237 ± 0.020

Remarkably, CIP is the first peroxidase reported to display more than two redox-linked protonating groups that change their pK_a values depending on the redox state of the heme iron. Thus, a similar analysis of horseradish peroxidase (isoenzyme C) and manganese peroxidase showed that two redox-linked residues fully accounted for the pH dependence of the redox properties (19, 25, 26). As in other peroxidases, all redox-linked groups observed in CIP displayed a decrease in pK_a upon heme reduction, suggesting that the removal of one electron from the heme iron brings about a situation that renders less easy the protonation of these residues. Such a feature is likely referable to an electrostatic effect because Fe(II) is less positive than Fe(III), even though we cannot rule out redox-linked structural change(s) that induce a pK_a shift in residues surrounding the heme pocket.

To extend this analysis, we carried out a similar pH dependence investigation of CO binding kinetics, which yielded the information on the right side of Scheme 1. Fig. 2 shows the pH dependence of CO association, and Fig. 3 displays the pH dependence of the CO dissociation kinetics for CIP and the D245N mutant. In both cases, Equation 2 was employed for the analysis, even though it must be stressed that, in the case of the CO association process, the pK_a values refer to the P(II) populations of Scheme 1, whereas for the CO dissociation process, pK_a values refer to the PL(II) populations. In this way, the two types of kinetic information allow a complete description of the proton-linked modulation of the right side of Scheme 1. However, because for the CO association kinetics, the populations coming into play (*i.e.* P(II)) are in common with those involved in the redox process reported above (*i.e.* P(II) and P(III)), we also tried to merge these two facts into a self-consistent fitting procedure to obtain from the two sets of data a minimum number of protonating groups accounting for the whole proton-linked equilibria involving the P(III), P(II), and PL(II) species for both CO kinetics and redox processes (Scheme 1).

Fig. 2*A* shows that an independent fitting of the CO association kinetic data for CIP could be undertaken using only two protonating residues, whose pK_a values are reported in Table II. If we compare them with values reported in Table I for the pH dependence of the redox equilibria, we notice that there is a substantial overlap between the $pK_{a2(red)}$ value in Table I (for $n = 3$) and the pK_{a1} value in Table II (for $n = 2$). On the other hand, the value of pK_{a2} for the kinetic proton linkage appears to be irreconcilable with any of the $pK_{a(red)}$ values reported for $n = 3$ in Table I, whereas it is fairly close to the $pK_{a4(red)}$ value for $n = 4$. Altogether, these observations seem to indicate that there is a partial overlap between proton-linked residues modulating redox properties and CO association kinetic parameters, such that Scheme 1 with four protons (*i.e.* $n = 4$) could be required for a complete description of the linkage between protons, redox equilibria, and CO binding behavior.

However, to find out in a more quantitative fashion whether

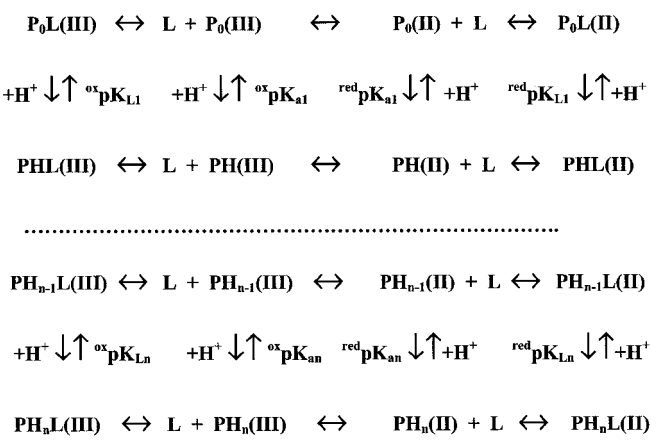

SCHEME 1. **General scheme for the redox-, ligand-, and proton-linked equilibria investigated in CIP.** *Horizontal* equilibria on the *left side* concern the redox processes. *Horizontal* equilibria on the *right side* refer to the ligand (L) binding in the reduced forms. *Vertical* equilibria refer to the protonation processes.

this is a reasonable assessment, we fitted the pH dependence of the CO association kinetics imposing the three $pK_{a(red)}$ values reported in Table I for $n = 3$ and allowing a free flotation of k_i values (Equation 2). Fig. 2*B* (– – –), corresponding to what was obtained by least-squares fitting of data according to this procedure, shows that these values are inadequate to give a satisfactory description of the pH dependence of the CO association kinetics because the transition at lower pH values, corresponding to the value of pK_{a2} for $n = 2$ (Table II), is missed. On the other hand, imposing values of $pK_{a(red)}$ for $n = 4$ in Table I (for redox potentials) gives a very satisfactory fitting of the pH dependence of the CO association kinetics (Fig. 2*B*, ——), supporting that four protons indeed are the minimum number required for the whole description of proton linkage for redox and kinetic properties, with two values overlapping (Table II for $n = 4$). As a self-consistent test, we also fitted the CO binding data employing Equation 2, leaving a free flotation of both k_i and $pK_{a(red)}$ values and obtaining a set of parameters closely similar (within the uncertainty limits) to those reported in Table II for $n = 4$.

A similar analysis was carried out for the pH dependence of the CO association kinetics of the D245N mutant; also in this case, two protonating groups were sufficient to give an independent description of the pH dependence (Fig. 2*A* and Table II for $n = 2$). Such pK_a values were very close to two of those obtained by analysis of the pH dependence of the redox properties for $n = 4$ (*viz.* $pK_{a2(red)}$ and $pK_{a3(red)}$) (Table I), but they were irreconcilable with the values obtained for the same analysis for $n = 3$ (Table I). This appears to be evident also comparing the fitting of the pH dependence of the CO association kinetics of D245N imposing $pK_{a(red)}$ values from the proton-linked behavior of redox potentials either for $n = 3$ (Fig. 2*C*,

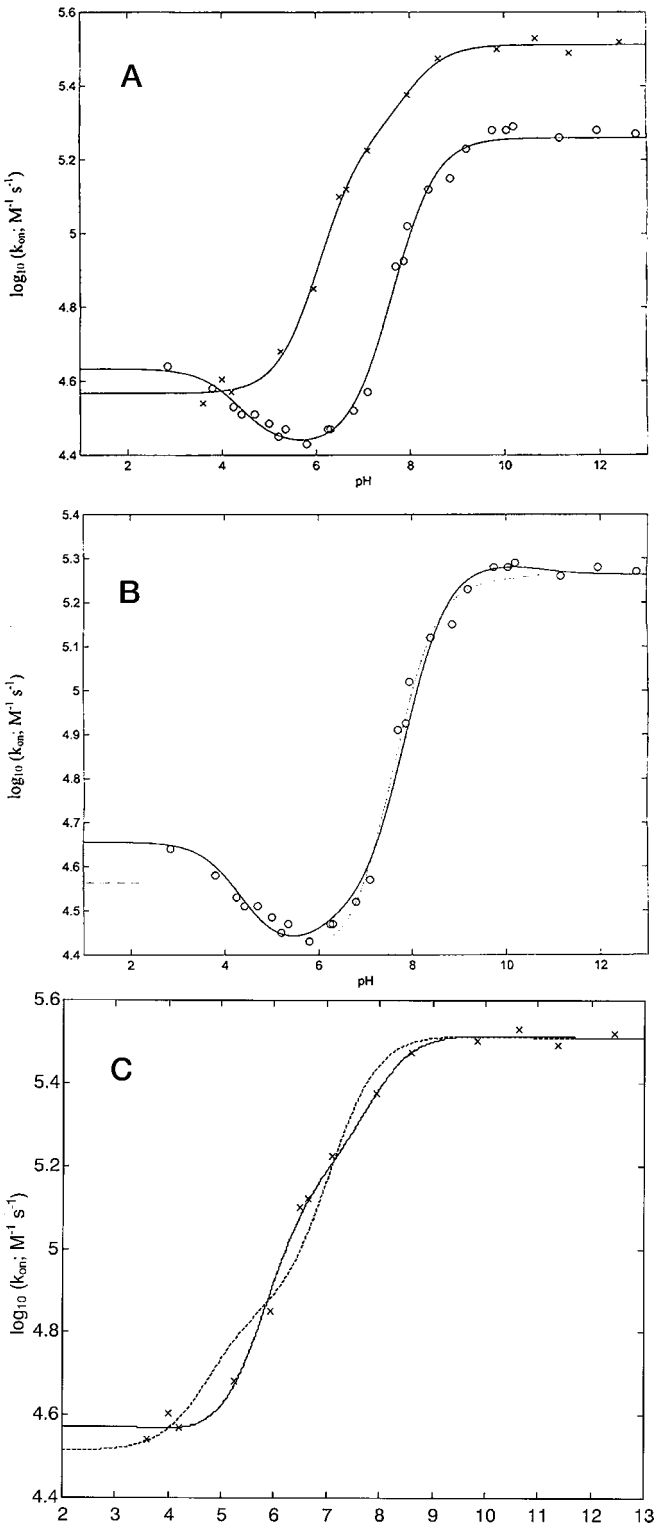

FIG. 2. *A*, pH dependence of the CO association rate constants for CIP (○) and D245N (×) at 25 °C. ——, nonlinear least-squares fitting of the data according to Equation 2 employing the values reported in Table II for $n = 2$. *B*, pH dependence of the CO association rate constant for CIP at 25 °C. – – –, nonlinear least-squares fitting of the data according to Equation 2 imposing values of $pK_{a(red)}$ for $n = 3$ (Table I); ——, nonlinear least-squares fitting of the data according to Equation 2 imposing values of $pK_{a(red)}$ for $n = 4$ (Table I). *C*, pH dependence of the CO association rate constant for D245N at 25 °C. - - - - -, nonlinear least-squares fitting of the data according to Equation 2 imposing values of $pK_{a(red)}$ for $n = 3$ (Table I); ——, nonlinear least-squares fitting of the data according to Equation 2 imposing values of $pK_{a(red)}$ for $n = 4$ (Table I). For further details, see "Results."

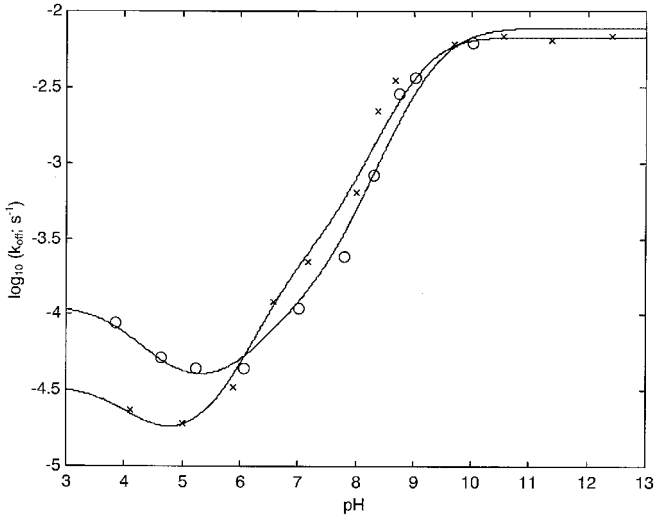

FIG. 3. **pH dependence of the CO dissociation rate constants for CIP (○) and D245N (×) at 25 °C.** ——, nonlinear least-squares fitting of the data according to Equation 2. Values of k_i and pK_{Li} are reported in Table III. The outcome of the fitting was constrained by mass law relationships with values of k_i and $pK_{a1(red)}$ reported in Table II, such as for each step i (Schemes 1–3), Equation 3 has been used to apply this constraint. For further details, see "Results."

TABLE II

Values of k_i and pK_a for the pH dependence of the CO association kinetics for CIP and D245N from the independent least-squares fitting of the data according to Equation 2 employing $n = 2$ and/or imposing values of $pK_{a(red)}$ from the proton-linked redox behavior reported in Table I ($n = 4$).

	CIP	D245N
$n = 2$		
k_1 (M^{-1} s^{-1})	$(1.82 \pm 0.21) \times 10^5$	$(3.25 \pm 0.42) \times 10^5$
k_2 (M^{-1} s^{-1})	$(2.64 \pm 0.28) \times 10^4$	$(1.82 \pm 0.24) \times 10^5$
k_3 (M^{-1} s^{-1})	$(4.30 \pm 0.51) \times 10^4$	$(3.69 \pm 0.43) \times 10^4$
pK_{a1}	8.05 ± 0.17	8.08 ± 0.18
pK_{a2}	4.29 ± 0.18	6.41 ± 0.17
$n = 4$		
k_1 (M^{-1} s^{-1})	$(1.83 \pm 0.20) \times 10^5$	$(3.24 \pm 0.41) \times 10^5$
k_2 (M^{-1} s^{-1})	$(1.94 \pm 0.22) \times 10^5$	$(3.30 \pm 0.42) \times 10^5$
k_3 (M^{-1} s^{-1})	$(3.16 \pm 0.33) \times 10^4$	$(1.53 \pm 0.23) \times 10^5$
k_4 (M^{-1} s^{-1})	$(2.58 \pm 0.27) \times 10^4$	$(3.55 \pm 0.45) \times 10^4$
k_5 (M^{-1} s^{-1})	$(4.53 \pm 0.54) \times 10^4$	$(3.74 \pm 0.47) \times 10^4$
$pK_{a1(red)}$ [a]	10.75	10.12
$pK_{a2(red)}$ [a]	8.24	7.97
$pK_{a3(red)}$ [a]	6.10	6.12
$pK_{a4(red)}$ [a]	4.21	4.31

[a] Fixed parameters.

- - - - -) and for $n = 4$ (Fig. 2*C*, ——). Therefore, as observed for CIP, the global description of the proton linkage to the redox properties and CO association kinetics of D245N requires four protonating groups, two of which are overlapping.

For the pH dependence of the CO dissociation kinetics (reported in Fig. 3) that lead to the determination of $pK_{L(red)}$ (Scheme 1), we followed a conceptually similar approach, even though it must be stressed that, in this case, our constraint was different from that used for the CO association kinetics because we have no independent determination of $pK_{L(red)}$ values. The constraint is instead related to the fact that the values of the association and dissociation kinetic constants at each protonation stage i and $i - 1$ (and thus the corresponding equilibrium constants) must be consistent with the values of $pK_{a1(red)}$ and $pK_{L1(red)}$ so as to obey mass conservation law within each thermodynamic square (Scheme 1), as for the following relationship (Equation 3).

$$(k_{i-1(off)}/k_{i(off)}) \cdot 10^{pK_{L1}} = (k_{i-1(on)}/k_{i(on)}) \cdot 10^{pK_{a1}} \qquad \text{(Eq. 3)}$$

TABLE III
Kinetic rate constants and protonation parameters for the CO dissociation from CIP and D245N

	CIP	D245N
k_1 (s^{-1})	$(7.73 \pm 0.63) \times 10^{-3}$	$(6.73 \pm 0.57) \times 10^{-3}$
k_2 (s^{-1})	$(7.73 \pm 0.36) \times 10^{-3}$	$(6.73 \pm 0.31) \times 10^{-3}$
k_3 (s^{-1})	$(1.18 \pm 0.27) \times 10^{-4}$	$(2.73 \pm 0.54) \times 10^{-4}$
k_4 (s^{-1})	$(3.29 \pm 0.09) \times 10^{-5}$	$(1.38 \pm 0.18) \times 10^{-5}$
k_5 (s^{-1})	$(1.14 \pm 0.07) \times 10^{-4}$	$(3.41 \pm 1.03) \times 10^{-5}$
$pK_{L1(red)}$	10.78 ± 0.17	10.13 ± 0.17
$pK_{L2(red)}$	9.27 ± 0.14	9.02 ± 0.19
$pK_{L3(red)}$	6.64 ± 0.15	6.84 ± 0.17
$pK_{L4(red)}$	4.06 ± 0.15	3.94 ± 0.16

In this way, the pH dependence of the redox equilibria and the CO association and dissociation kinetic rate constants all become functionally interrelated through a set of proton linkage relationships, giving rise to a complete description of the modulation of the whole system. Therefore, to be consistent with what was already determined for the proton linkage of the redox and CO association kinetic behavior, analysis of the pH dependence of the CO dissociation kinetics was limited to the search for a set of five dissociation rate constants (corresponding to the 0–4 protonated species) and four $pK_{L(red)}$ values that altogether obey the mass law constraints described above. Despite the large number of parameters involved, the limitations imposed turned out to be fairly restrictive, as essentially only one solution was found for CIP and D245N that satisfactorily described the pH-dependent behavior of their CO dissociation kinetics (Fig. 3 and Table III).

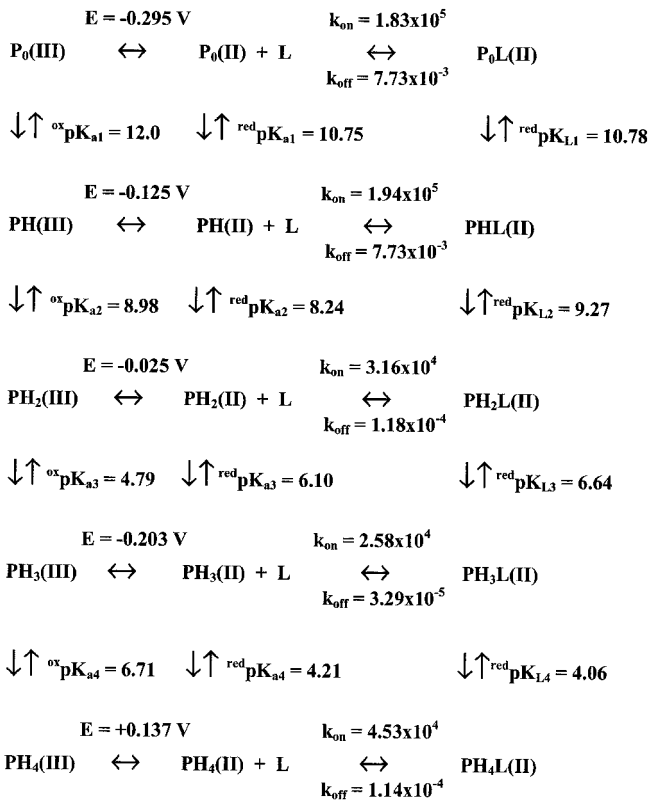

SCHEME 2. **Overall redox-, ligand-, and proton-linked equilibria of CIP.**

DISCUSSION

The overall description of the pH dependence of the redox properties and CO association and dissociation kinetics of CIP can be fully accounted for by the redox- and ligand-linked protonation of four groups, and this behavior is depicted in Schemes 2 and 3 for CIP and D245N, respectively. An important observation is that, unlike for other peroxidases investigated up to now, the observed pH dependence cannot be accounted for by only two redox-linked groups, suggesting that CIP shows a different environment of the heme pocket compared with other peroxidases, bringing about a variation of the protonation properties of residues that affect the redox properties, with the involvement of additional redox-linked group(s). However, it must be stressed that it is the first time (at least to our knowledge) that an attempt has been undertaken to merge in a systematic way the redox, ligand binding, and proton linkage information on a peroxidase. Therefore, we cannot rule out the possibility that such an investigation on other peroxidases will give a similar outcome.

In particular, a comparative study has been carried out between wild-type cytochrome *c* peroxidase and the side-directed mutant D235N for CO association and dissociation kinetics (27, 28), but it was extended over a much more limited pH range. In any case, the behavior observed was qualitatively similar to what was observed in CIP and D245N because the CO association rate constant was ~5-fold faster in the case of the D235N mutant with respect to wild-type cytochrome *c* peroxidase (27), whereas a closely similar CO dissociation rate constant was observed, which, in both proteins, displayed a decrease as the pH was lowered (28).

An additional step to understand from the structural standpoint how redox properties and ligand binding features are modulated in CIP and D245N is to try to identify the four protonating groups or at least to give some hint as to which might be the most plausible candidates to play different proton-linked roles. Although this is not easy, some insight can be obtained by the investigation of the redox properties in the site-directed mutant D245N because the substitution of Asp^{245} with Asn weakens the H-bond between the carboxylate of Asp^{245} and N^{δ} of the proximal His^{183}, likely affecting proton-linked equilibria. We first noticed that one of these residues, *viz.* pK_{a1}, was greatly affected by the mutation, which also significantly influenced pK_{a2}, whereas pK_{a3} remained unchanged, and pK_{a4} was only slightly altered by the mutation (Table I). In particular, it is very informative that the substitution of Asp^{245} with Asn brought about a lower value for pK_{a1} both in the oxidized ($pK_{a1(ox)}$ = 10.74 ± 0.13 in D245N and 12.00 ± 0.14 in CIP) and in the reduced ($pK_{a1(red)}$ = 10.12 ± 0.12 in D245N and 10.75 ± 0.13 in CIP) forms, indicating that the much weaker H-bond and the consequent structural change(s) induce a relevant decrease in the protonation features of this residue such that it protonates less easily (Table I). Similar considerations apply to the effect of the substitution on pK_{a2}, even though in this case the shifts in pK_a values were smaller than for the group characterized by pK_{a1} (Table I). Thus, upon heme reduction, the pK_{a2} values shifted from 8.98 ± 0.15 to 8.24 ± 0.17 in CIP and from 8.65 ± 0.16 to 7.97 ± 0.17 in D245N. On the other hand, the residue responsible for pK_{a1} showed almost no effect on the CO association kinetics for both CIP and D245N (Schemes 2 and 3 and Table II), and the same is true for pK_{L1} on the CO dissociation kinetics (Schemes 2 and 3 and Table III). As a whole, such features might suggest that the residue responsible for pK_{a1} is a very basic residue. It may be interesting to recall that, over the same pH range, a spectroscopic transition has been reported to occur in the ferric resting state of CIP and D245N, which has been assigned to the binding of the hydroxyl ion to Fe(III) (21, 22). This occurrence appears to be associated with the weakening of the proximal Fe–His^{183} bond, and it displays a higher pK_a value in CIP than in D245N (as also observed in our case for $pK_{a1(ox)}$) (Table I)), a difference that must be associated with a different interaction mode of OH^- with residues of the distal portion of the heme pocket (21, 22). The observed values of pK_a

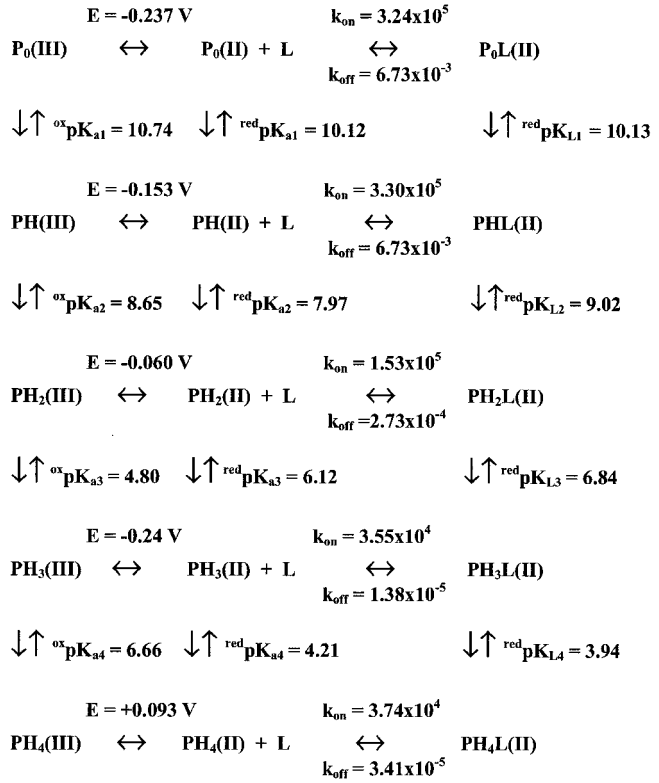

SCHEME 3. **Overall redox-, ligand-, and proton-linked equilibria of D245N.**

for the formation of the Fe(III)–OH^- adduct in CIP and D245N (21, 22) are compatible with the values of $pK_{a1(ox)}$ reported in Table I, suggesting that they likely refer to the same phenomenon. In addition, also the Fe(II) form of both proteins displayed a spectroscopic transition over the same pH range (Fig. 4*A*), suggesting a conformational change from a pentacoordinated species to a hexacoordinated one, with pK_a values significantly different between CIP (pK_a = 11.70 ± 0.12) and D245N (pK_a = 10.68 ± 0.13) (Fig. 4*B*). It must be remarked that the pK_a values for the spectroscopic transition of the unliganded Fe(II) forms are different from the $pK_{a1(red)}$ values reported in Table I for the two proteins, clearly indicating that they do not refer to the same phenomenon, even though it appears evident that they seem related because they have a closely similar trend. Altogether, these observations may suggest that the group responsible for the most alkaline transition, corresponding to pK_{a1}, is N^{δ} of the proximal His^{183}. Thus, the occurrence of the H-bond of this group with Asp^{245} in CIP is likely to bring about a very high pK_{a1} value, which is significantly decreased upon the drastic weakening of the H-bond in the D245N mutant. This assignment is also consistent with the observation that the deprotonation of this residue induces the formation of a hexacoordinated species. As a matter of fact, the H-bond holds the proximal imidazole, which is thus constrained in a well defined conformation; the deprotonation of N^{δ} is then very likely associated with an increase in the degrees of freedom for the proximal imidazole, decreasing the energy barrier for its movement toward the heme plane and thus facilitating the hexacoordination. Therefore, the severe weakening of this H-bond in D245N likely decreases the pK_a value for the protonation of N^{δ} of His^{183}, thus facilitating also the hexacoordination.

Lowering the pH from 10 to 6 brought about in both CIP and D245N an almost 10-fold reduction in the observed second-order rate constant for CO binding (Fig. 2), which was accompanied by a 100-fold decrease in the CO dissociation rate constant (Fig. 3), resulting in a pH-dependent increase in CO

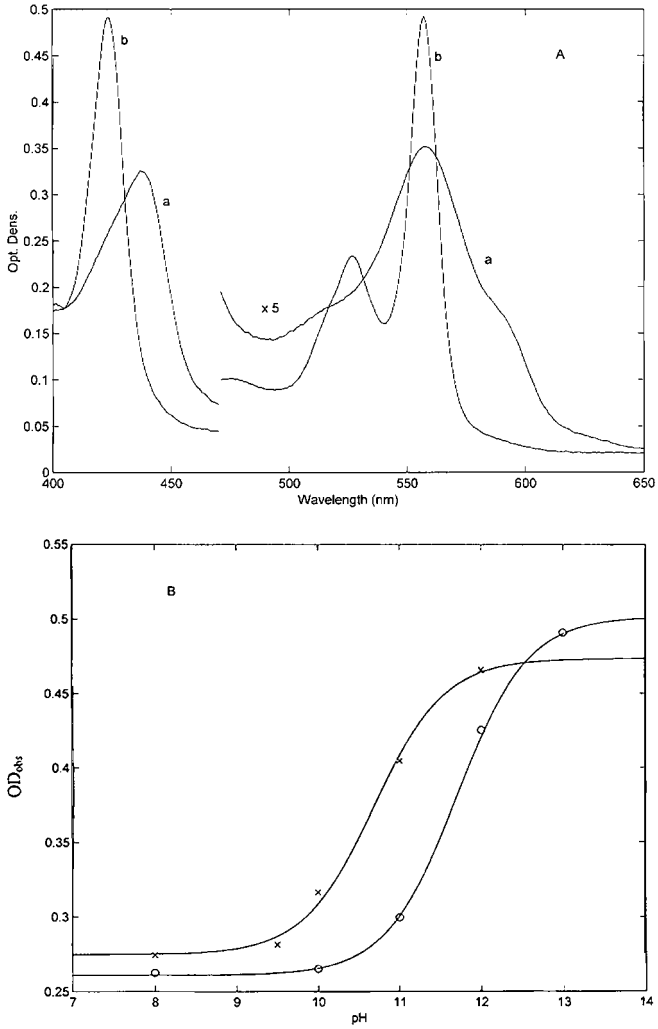

FIG. 4. *A*, absorption spectra of the unliganded Fe(II) form of CIP at pH 8.0 (*spectrum a*) and 13.0 (*spectrum b*). Absorption spectra in the visible region were multiplied by 5. Similar spectral changes were observed for the unliganded Fe(II) form of D245N. *B*, pH dependence of the absorption at λ = 423 nm for the unliganded Fe(II) forms of CIP (○) and D245N (×) at 25 °C. ——, least-squares fitting of the experimental data according to the following equation, $A_{obs} = A_0 + \Delta A \cdot (K_a \cdot [H]^+ / (1 + K_a \cdot [H]^+))$, where A_{obs} is the observed absorbance at λ = 423 nm at a given pH, A_0 is the absorbance at the lowest limit of the pH values, ΔA is the total absorbance change corresponding to the pH-dependent transition, K_a is the proton binding constant (10^{pK_a}), and $[H^+]$ is the proton concentration (10^{-pH}). For further details, see "Discussion."

binding equilibrium affinity (which is much more marked than in the case of cytochrome *c* peroxidase (27, 28)). For the CO association process, such a transition appears to be modulated mostly by $pK_{a2(red)}$ in CIP and by $pK_{a3(red)}$ in D245N (Schemes 2 and 3 and Table II). On the other hand, the CO dissociation rate constant was modulated by both $pK_{L2(red)}$ and $pK_{L3(red)}$ in both CIP–CO and D245N–CO (Table III). The assignment of the residue responsible for pK_{a2}, which plays a relevant proton-linked modulatory role in the redox properties as well as in CO association with CIP (but not with D245N) and in CO dissociation from both CIP and D245N (Schemes 2 and 3), is, however, not obvious. The values of both $pK_{a2(red)}$ and $pK_{L2(red)}$ were affected to a similar extent by the weakening of the H-bond, showing a ≈0.25-pH unit shift between CIP and D245N (Schemes 2 and 3). As a matter of fact, there are several groups in close proximity that might show a value of pK_a within the pK_{a2} range; the most likely one might be one of the two water molecules bridging one of the propionates with Arg^{51} (Fig. 5)

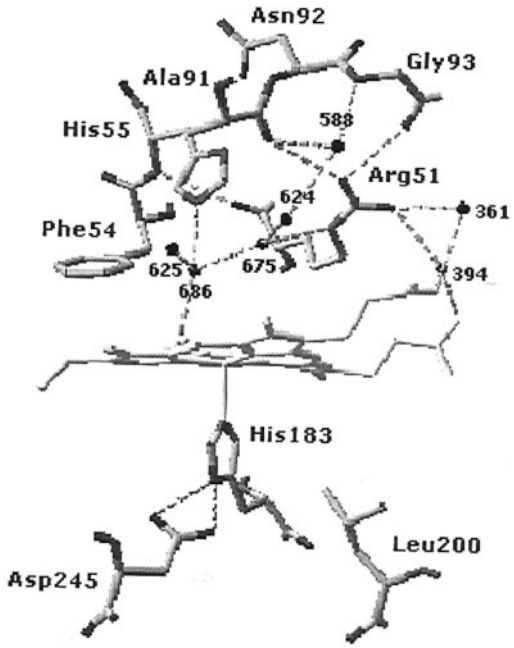

FIG. 5. **Structural diagram of the heme pocket of CIP according to the crystal structure of Ref. 20.** Key residues of heme surroundings are indicated. Seven distal water molecules in the heme-linked H-bond network are also shown (*black spheres*). The image was generated using the Swiss-PdbViewer Version 3.7 visualization program. For further details, see "Discussion."

(14, 20). Thus, the close proximity with the negative charge of the propionate could give this H_2O molecule(s) a strong ionic character with a very high pK_a value. Furthermore, its location renders it very likely that the oxidation state of the heme iron has a relevant effect on the pK_a value of such an H-bond network, and the same can be true for the CO-bound form. This being true, it may be very likely that the alteration of the heme geometry, induced by the severe weakening of the proximal H-bond in D245N, brings about a variation of the interaction between the propionate and Arg^{51} (mediated by this H_2O molecule) and thus a decrease in the pK_a value and/or a displacement of Arg^{51} such that it plays a less important role in the modulation of CO association in favor of the residue responsible for pK_{a3} (see above).

On the other hand, the identification of the residue responsible for pK_{a3} appears to be less problematic because its proton-linked redox behavior leads to its identification as the distal His^{55}. Thus, the value of p$K_{a3(ox)}$ is very low, as has been indicated by several observations to be the case for the distal His in peroxidases (29), displaying a remarkable pK_a increase upon reduction of the heme iron. This behavior might suggest that the environment of the distal His^{55} changes significantly when Fe(III) is reduced to Fe(II), possibly because of a structural movement of Arg^{51}, which has been thought to be mainly responsible (with its positive charge) for the very low pK_a value displayed by His^{55} in the Fe(III) species (29). Conversely, the mutation that occurs on the proximal side upon the substitution of Asp^{245} with Asn does not seem to affect at all the p$K_{a3(ox)}$ and p$K_{a3(red)}$ values, indicating that the environment of His^{55} is not perturbed by this mutation. Unfortunately, site-directed mutants of His^{55} are not available for CIP to prove that this assignment is true, but under this very reasonable assumption, it appears that His^{55} indeed is an important modulator of CO binding to D245N, turning out to be much less crucial in the case of CIP. This clearly indicates that the mutation that occurs on the proximal side, which brings about the severe weakening of the H-bond, induces a conformational change that is transmitted also to the distal side of the heme pocket, rendering much more important the functional role of His^{55} in CO binding (or else reducing the role played by some other determinant, such as that characterized by p$K_{a2(red)}$). In this respect, it can be emphasized that the faster CO binding rate constant of D245N with respect to CIP can be fully attributed to a decrease in the energy barrier for ligand access to the heme, an observation that indeed confirms that the mutation that occurs in D245N alters the shield between the bulk solvent and the heme. However, this structural change does not appear to affect the ionic properties of His^{55}, which maintains unchanged pK_a values (Schemes 2 and 3 and Table I), but instead of some other residue(s), such as the one(s) characterized by pK_{a2}, whose role in CO binding is drastically reduced in D245N, this being also associated with a variation of pK_a values in the mutant (Schemes 2 and 3 and Tables I and II). On the other hand, this assignment being true, His^{55} seems to play a main role in the control of the CO dissociation from both CIP–CO and D245N–CO, suggesting that the conformational change mainly affects the unliganded Fe(II) form.

In the case of the residue responsible for p$K_{a4(red)}$, it must be noted that its protonation appears to have an accelerating effect on the CO association with CIP, whereas in D245N, although showing a closely similar value (Schemes 2 and 3), it has almost no effect on the analogous process. On the other hand, the protonation of this residue, being characterized by pK_{L4} (with values lower than the corresponding p$K_{a4(red)}$ values) in the CO-bound form, has a similar effect on the CO dissociation from both CIP and D245N. This behavior and the p$K_{a4(red)}$ and pK_{L4} values suggest that this residue is likely N^{ϵ} of the imidazole of the proximal His^{183}, which is involved in the proximal axial bond. This being correct, the raising of the observed CO dissociation rate constant as pH is decreased below 6 (for CIP) and 5 (for D245N) (Fig. 3) is directly related to the appearance of the pentacoordinated CO complex. This assignment, which implies that the protonation event is associated with the weakening of the proximal bond, appears to be consistent with spectroscopic observations by electronic absorption, resonance Raman spectroscopy, and NMR (21, 22). Furthermore, the p$K_{a4(ox)}$ value, measured from the pH dependence of the redox properties (Fig. 1 and Table I), is closely similar to the value determined independently for the ferric form of CIP (30).

As a whole, this analysis allows us to envisage a general mechanism for the linkage among protons, ligand binding, and redox equilibria where four protons are required for an overall description of both CIP and D245N, with different effects that also point out the role of the H-bond between Asp^{245} and N^{δ} of the proximal His^{183}. First of all, the severe weakening of the proximal H-bond in D245N brings about an alteration of pK_a for two of the four redox-linked protonating residues (likely being N^{δ} of His^{183} and an H_2O-bound network of charges in the distal side of the heme pocket) (Schemes 2 and 3). Furthermore, although three of the four redox-linked protonating groups are also ligand-linked for both CIP and D245N (Schemes 2 and 3), the kinetic effects are different in the two molecules, reflecting the alteration that occurs on the distal side of the heme pocket as a consequence of the weakening of the proximal H-bond in D245N. Thus, the role played by the H_2O-bound network of charges, which is predominant in CIP, is overwhelmed in D245N by the role of His^{55}, and this is likely referable to a structural change that occurs in the distal side upon the mutation in the proximal portion of the heme pocket (and possibly involving Arg^{51} and the H_2O-mediated bridge with one of the heme propionates). In addition, the drastic weakening of the proximal H-bond seems to alter the kinetic control of CO bind-

ing by the proximal axial bond of the heme, corresponding to the protonation of N^{ϵ} of His^{183} (see $pK_{a4(red)}$ in Schemes 2 and 3), because, unlike for CIP, no effect is observed on CO binding to D245N upon protonation of the residue characterized by $pK_{a4(red)}$ (Scheme 3). However, it must be pointed out that, in peroxidases, the role of this protonation in the modulation of CO binding is significantly reduced with respect to myoglobins and hemoglobins, where the protonation of N^{ϵ} of the proximal histidine is associated with a large increase in the CO binding rate constant (7, 31). This behavior might be correlated, at least in CIP and D245N, with the fact that the stereochemical arrangement of the heme is held in a more fixed position, which renders the intrinsic reactivity with CO more favorable and less influenced by the protonation of the proximal imidazole. In conclusion, CIP appears to display a much tighter connection between the proximal and distal sides of the heme pocket with respect to other peroxidases such as horseradish peroxidase (isoenzyme C) and manganese peroxidase (as already outlined by spectroscopic observations (21 and 22)), and this appears to be particularly evident in that the weakening of the proximal H-bond brings about a conformational transition on the distal side of the heme pocket that renders faster access of the ligand to the heme pocket.

Acknowledgments—We thank Prof. G. Smulevich and Dr. A. Feis for several stimulating discussions and Novozymes Co. for the recombinant wild-type and mutant proteins.

REFERENCES

1. Unzai, S., Eich, R., Shibayama, N., Olson, J. S., and Morimoto, H. (1998) *J. Biol. Chem.* **273,** 23150–23159
2. Gibson, Q. H. (1999) *Biochemistry* **38,** 5191–5199
3. Perutz, M. F. (1989) *Q. Rev. Biophys.* **22,** 139–237
4. Lambright, D. G., Balasubramanian, S., Decatur, S. M., and Boxer, S. G. (1994) *Biochemistry* **33,** 5518–5525
5. Brunori, M. (2000) *Biophys. Chem.* **86,** 221–230
6. Scott, E. E., Gibson, Q. H., and Olson, J. S. (2001) *J. Biol. Chem.* **276,** 5177–5188
7. Coletta, M., Ascenzi, P., Traylor, T. G., and Brunori, M. (1985) *J. Biol. Chem.* **260,** 4151–4155
8. Murray, L. P., Hofrichter, J. H., Henry, E. R., Ikeda-Saito, M., Kitagishi, K., Yonetani, T., and Eaton, W. A. (1988) *Proc. Natl. Acad. Sci. U. S. A.* **85,** 2151–2155
9. Decatur, S. M., Belcher, K. L., Rickert, P. K., Franzen, S., and Boxer, S. G. (1999) *Biochemistry* **38,** 11086–11092
10. Finzel, B. C., Poulos, T. L., and Kraut, J. (1984) *J. Biol. Chem.* **259,** 13027–13036
11. Poulos, T. L., Edwards, S. L., Wariishi, H., and Gold, M. H. (1993) *J. Biol. Chem.* **268,** 4429–4440
12. Sundaramoorthy, M., Kishi, K., Gold, M. H., and Poulos, T. L. (1994) *J. Biol. Chem.* **269,** 32759–32767
13. Kunishima, N., Fukuyama, K., Matsubara, H., Hatanaka, H., Shibano, Y., and Amachi, T. (1994) *J. Mol. Biol.* **235,** 331–344
14. Petersen, J. F. W., Kadziola, A., and Larsen, S. (1994) *FEBS Lett.* **339,** 291–296
15. Gajhede, M., Schuller, D. J., Henriksen, A., Smith, A. T., and Poulos, T. L. (1997) *Nat. Struct. Biol.* **4,** 1032–1038
16. Welinder, K. G. (1992) *Curr. Opin. Struct. Biol.* **2,** 383–393
17. Welinder, K. G., Bjørnholm, B., and Dunford, H. B. (1995) *Biochem. Soc. Trans.* **23,** 257–262
18. Mukai, M., Mills, C. E., Poole, R. K., and Yeh, S.-R. (2001) *J. Biol. Chem.* **276,** 7272–7277
19. Santucci, R., Bongiovanni, C., Marini, S., Del Conte, R., Tien, M., Banci, L., and Coletta, M. (2000) *Biochem. J.* **349,** 85–90
20. Fukuyama, K., Itakura, H., Sato, K., Takahashi, S., and Hosoya, T. (1997) *J. Biol. Chem.* **272,** 5752–5756
21. Smulevich, G., Neri, F., Marzocchi, M. P., and Welinder, K. G. (1996) *Biochemistry* **35,** 10576–10585
22. Veitch, N. C., Gao, Y., and Welinder, K. G. (1996) *Biochemistry* **35,** 14370–14380
23. Neri, F., Indiani, C., Welinder, K. G., and Smulevich, G. (1998) *Eur. J. Biochem.* **251,** 830–838
24. Welinder, K. G., and Andersen, M. B. (December 9, 1993) U. S. Patent WO93/24618
25. Ferri, T., Poscia, A., and Santucci, R. (1998) *Bioelectrochem. Bioenerg.* **44,** 177–181
26. Harbury, H. A. (1957) *J. Biol. Chem.* **225,** 1009–1024
27. Miller, M. A., Coletta, M., Mauro, J. M., Putnam, L. D., Farnum, M. F., Kraut, J., and Traylor, T. G. (1990) *Biochemistry* **29,** 1777–1791
28. Miller, M. A., Mauro, J. M., Smulevich, G., Coletta, M., Kraut, J., and Traylor, T. G. (1990) *Biochemistry* **29,** 9978–9988
29. Dunford, H. B. (2001) *J. Biol. Inorg. Chem.* **6,** 819–822
30. Abelskov, A. K., Smith, A. T., Rasmussen, C. B., Dunford, H. B., and Welinder, K. G. (1997) *Biochemistry* **36,** 9453–9463
31. Coletta, M., Ascenzi, P., and Brunori, M. (1988) *J. Biol. Chem.* **263,** 18286–18289